Supplement of Atmos. Chem. Phys., 25, 15953–15968, 2025
https://doi.org/10.5194/acp-25-15953-2025-supplement

Atmospheric Chemistry and Physics
Open Access

Supplement of

Chemical characterization and source apportionment of fine particulate matter in Kigali, Rwanda, using aerosol mass spectrometry

Theobard Habineza et al.

Correspondence to: Albert A. Presto (apresto@andrew.cmu.edu)

S1. Sampling location

The sampling location is situated at latitude -1.9619 and longitude 30.0645, at an altitude of about 1500 meters above sea level within Kigali City, Nyarugenge District, Rwanda. This site lies within the Intertropical Convergence Zone (ITCZ), where the sun rises around 6:00 AM and sets around 6:00 PM throughout the year. The weather conditions at this site are moderate across all seasons, with an annual average temperature ranging from 17°C to 24°C countrywide (Climatology of eastern Africa, 2025).

The rainfall pattern in this region is characterized by four alternating seasons: Two dry seasons: June–August (JJA) and December–February (DJF). Two rainy seasons: March-May (MAM) and September–November (SON). The annual mean precipitation at this site ranges between 1,100 mm and 1,300 mm, as it is in the central part of the country(The World Bank Group., 2021).

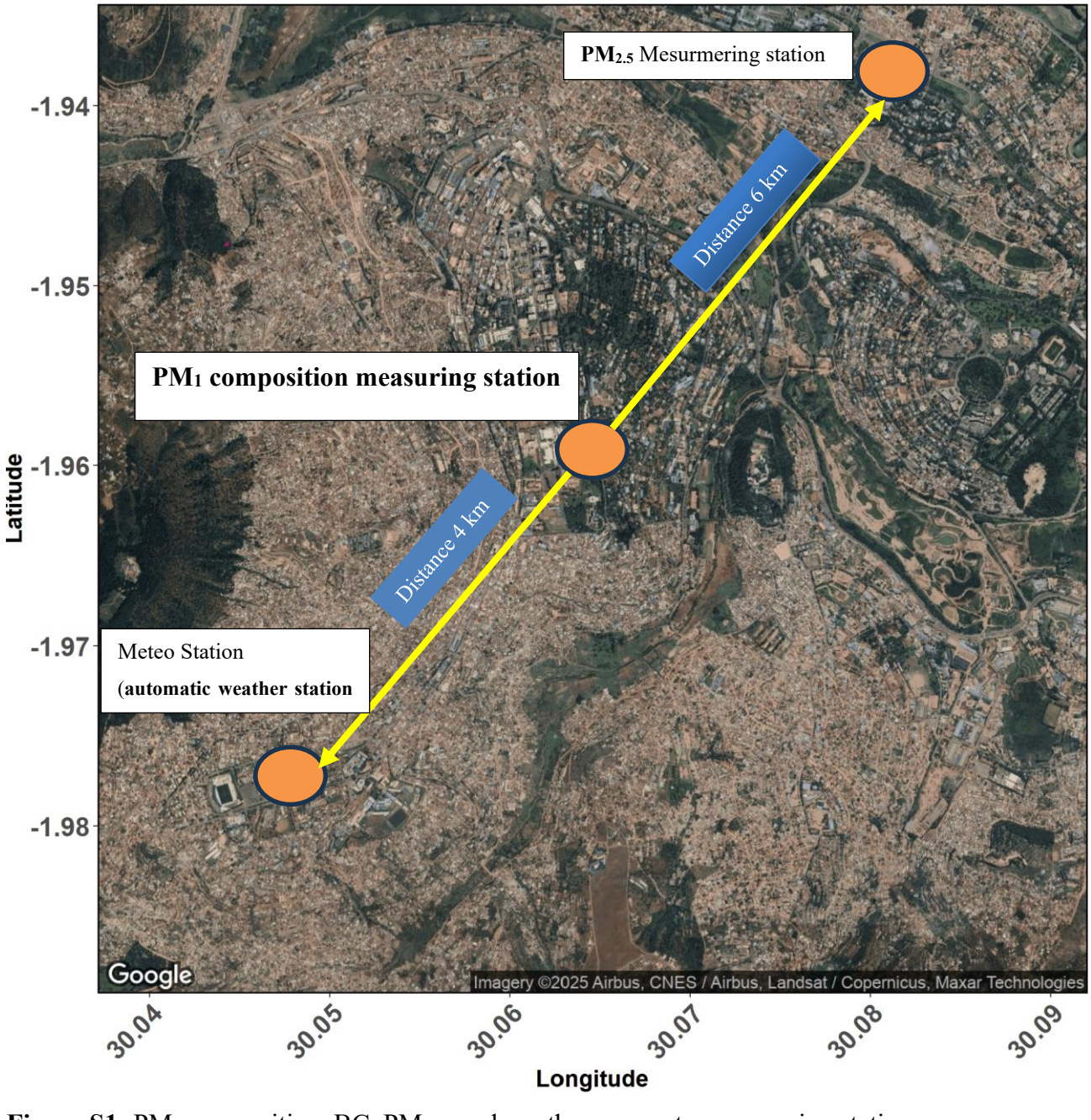

Figure S1: PM_1 composition, BC, $PM_{2.5}$**,** and weather parameters measuring stations**.**

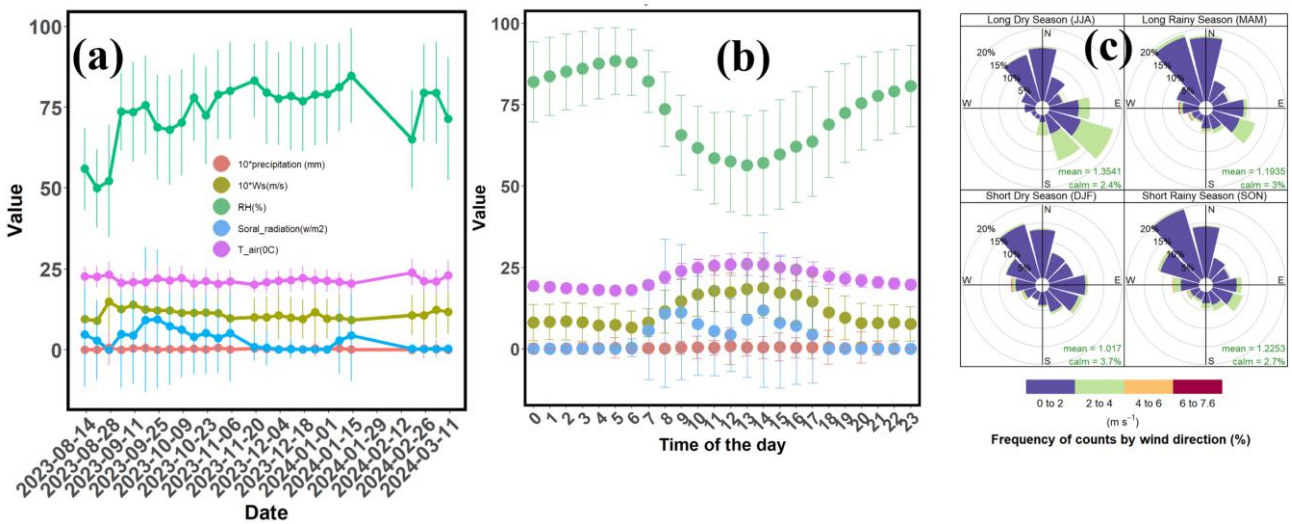

Figure S2: Weather parameter recorded at Kivugiza station, approximately 4 km from the monitoring site.: panel (a) shows weekly mean ± sd values. (b) shows the hourly mean diurnal patterns and (c) show the season wind roses.

A wind rose and diurnal plot diagram for the wind measured 2 meters in height along with the direction frequency across four seasons obtained at Kivugiza meteorological station from May 2023 to May 2024 shows that winds predominantly come from the north and northwest. Wind speeds mostly range between 0–4 m/s, with the strongest winds occurring during the Long Dry Season (JJA, mean = 1.35 m/s) and the weakest in the Short Dry Season (DJF, mean = 1.02 m/s, calm = 3.7%). The long rainy season (MAM, mean = 1.19 m/s) and short rainy season (SON, mean = 1.22 m/s) show moderate wind activity. Higher wind speeds above 4 m/s are rare. Overall, winds remain moderate throughout the year.

PM_1 vs $PM_{2.5}$ and annual mean diurnal variability in PM_1 components.

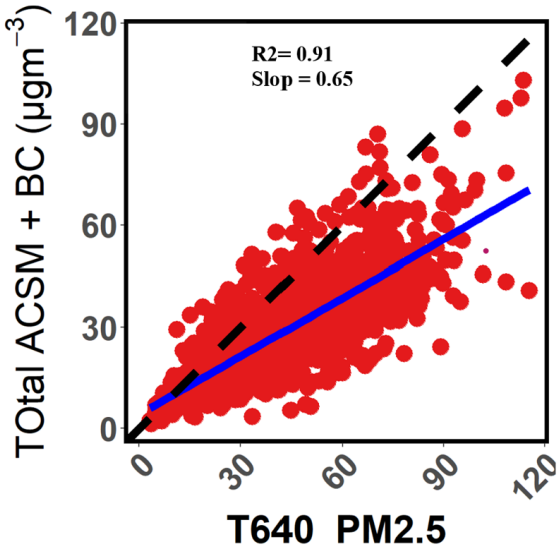

Figure S3: Comparison of PM_1 (NR_PM1+BC) with $PM_{2.5}$ measured at the US Embassy located 6 km from the sampling site

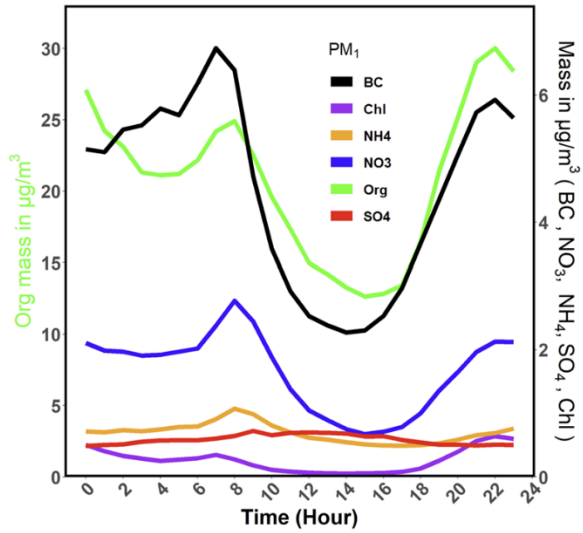

Figure S4: Annual mean diurnal pattern for the PM_1 components (SO_4, Org, NO_3, NH_4,Chl) and BC Organic aerosol (OA) concentrations are shown on the left y-axis, while all other species are plotted on the right y-axis.

S2. Particle organic nitrate vs inorganic nitrate.

Particle nitrate can be quantified using the approach developed by Fry et al.(2009). in Equation S1(Fry, 2009)

$$f_{pOrgNo3} = \frac{(R_{ambient} - R_{pNO3}) * (1 + R_{porgNO3})}{(R_{porgNO3} - R_{pNH_4NO_3}) * (1 + R_{ambient})} \quad \text{(S1)}$$

With the $R_{porgNO3}$ *can be* 0.1 (Farmer et al., 2010) *or infered* inferred as R_{pNO3}/RoR (Day et al., 2022) and the absence of standard $porgNO3$ value RoR = 2.75 ± 0.75**.** Figure below examines the three options to quantify the fraction on of Particle Nitrate is organic

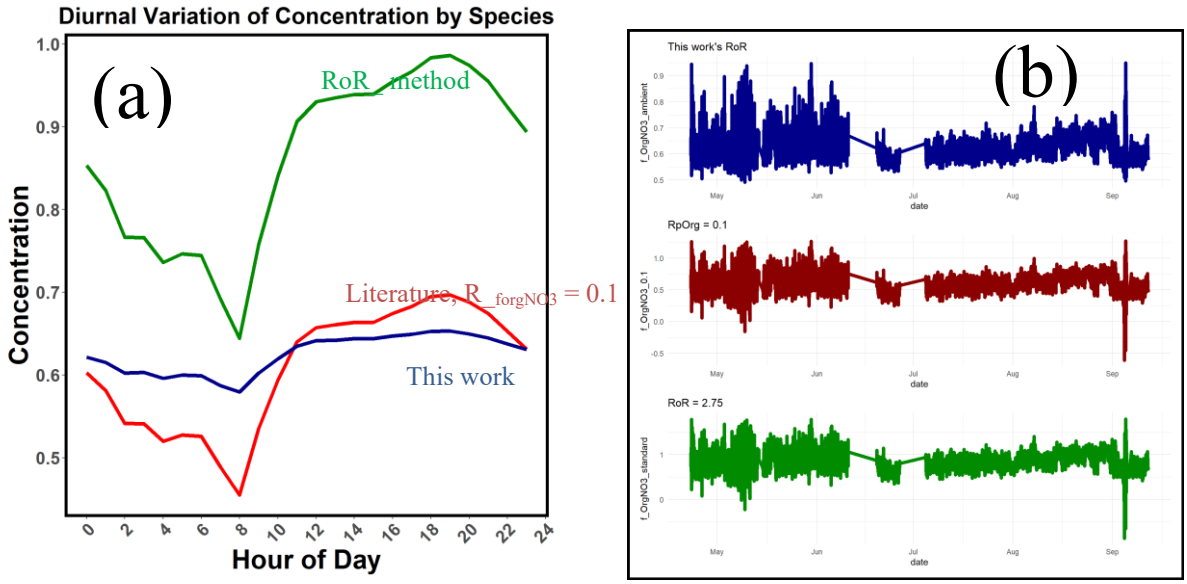

Figure S5: PM_1 particle-phase organic nitrate fraction. Panel (a) shows Diurnal patterns of the particle-phase organic nitrate fraction calculated using the ambient ratio (R_ambient; blue), the ratio-of-ratios (RoR) method (green), and a literature value of R_forgNO3 = 0.1 (red). Panel (b) shows the time series of the particle-phase organic nitrate fraction estimated using the standard RoR method, a literature R_pOrg = 0.1, and ratios calculated from ambient data (R_ambient).

At this site, we examined both quantification approaches, and Figure S5 illustrates the results. The calculated NO_2^+/NO^+ ratios as follows: $R_{porgNO3}$ = 0.56 ± 0.83, $R_{\_ambient}$ = 0.25 ± 0.06) and RoR = 2.5 ± 1.05 respectively. Using the calculated $R_{\_ambient}$, we estimated the average particle-phase organic nitrate fraction to be 61% ± 17% and no instance where $f_{pOrgNo3}$ exceeded 100%. Using Werden et al. (assuming $R_{porgNO3}$ = 0.1) method, we estimated the average $f_{pOrgNo3}$ of 61% ± 14.6% and during some instances of $f_{pOrgNo3}$ exceeding 100%. In contrast, using the method from Day et al. (RoR = 2.7 ± 0.75), the particle organic nitrate fraction counted for 98% ± 23.5%, and in most of the time $f_{pOrgNo3}$ exceeded 100%, indicating overestimation (Figure S5). Given the consistency of the Werden-based estimate and

the ambient ratio method with the unrealistic output from the Day et al. method, we adopted ambient ratios that accounts for the instrument performance over time. This supports the conclusion that, on average, 61% of the nitrate in Kigali is organic, while the remaining 39% is present as inorganic ammonium nitrate.

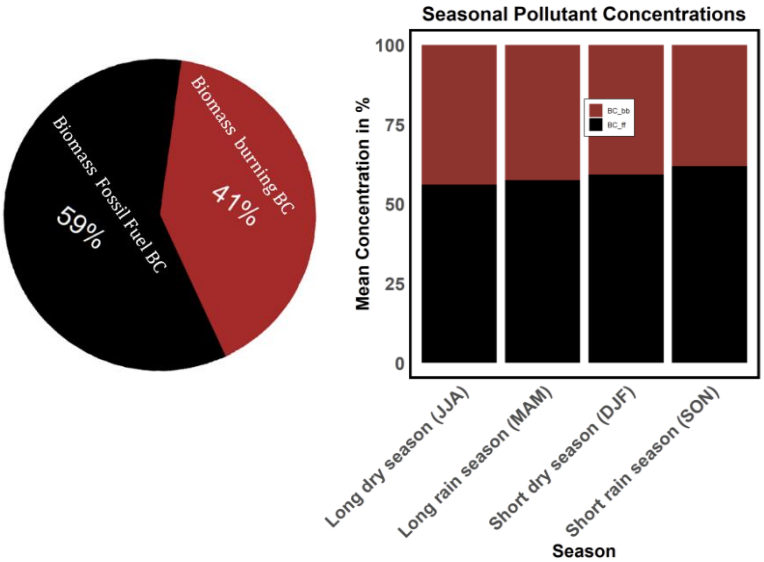

Figure S6: Overall (left) and seasonal (right) attribution of BC due to fossil fuel and biomass burning sources.

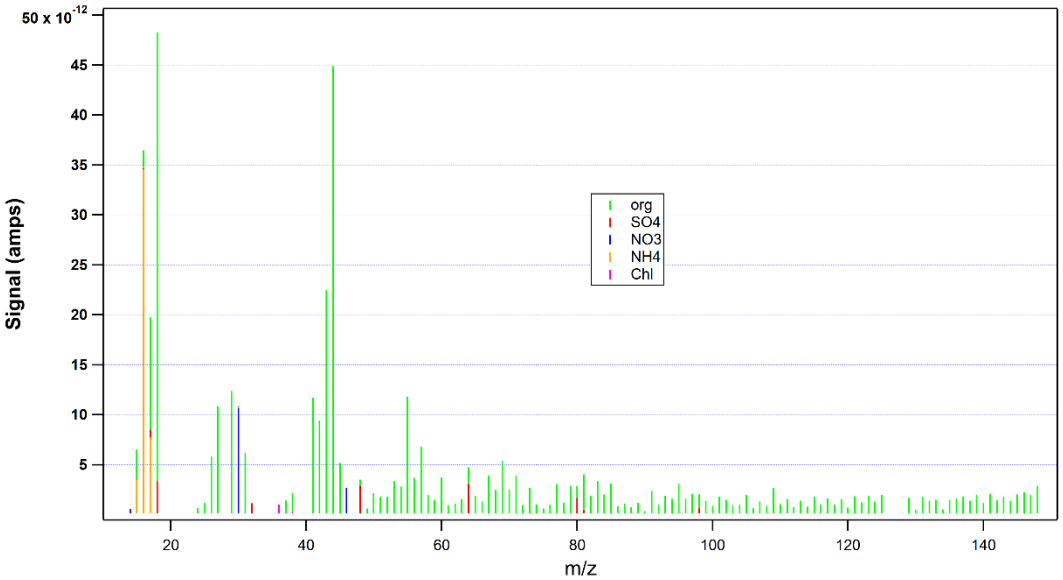

Figure S7: Annual average ambient mass spectra from the Q-ACSM

S3. PMF output and diagnostic plots

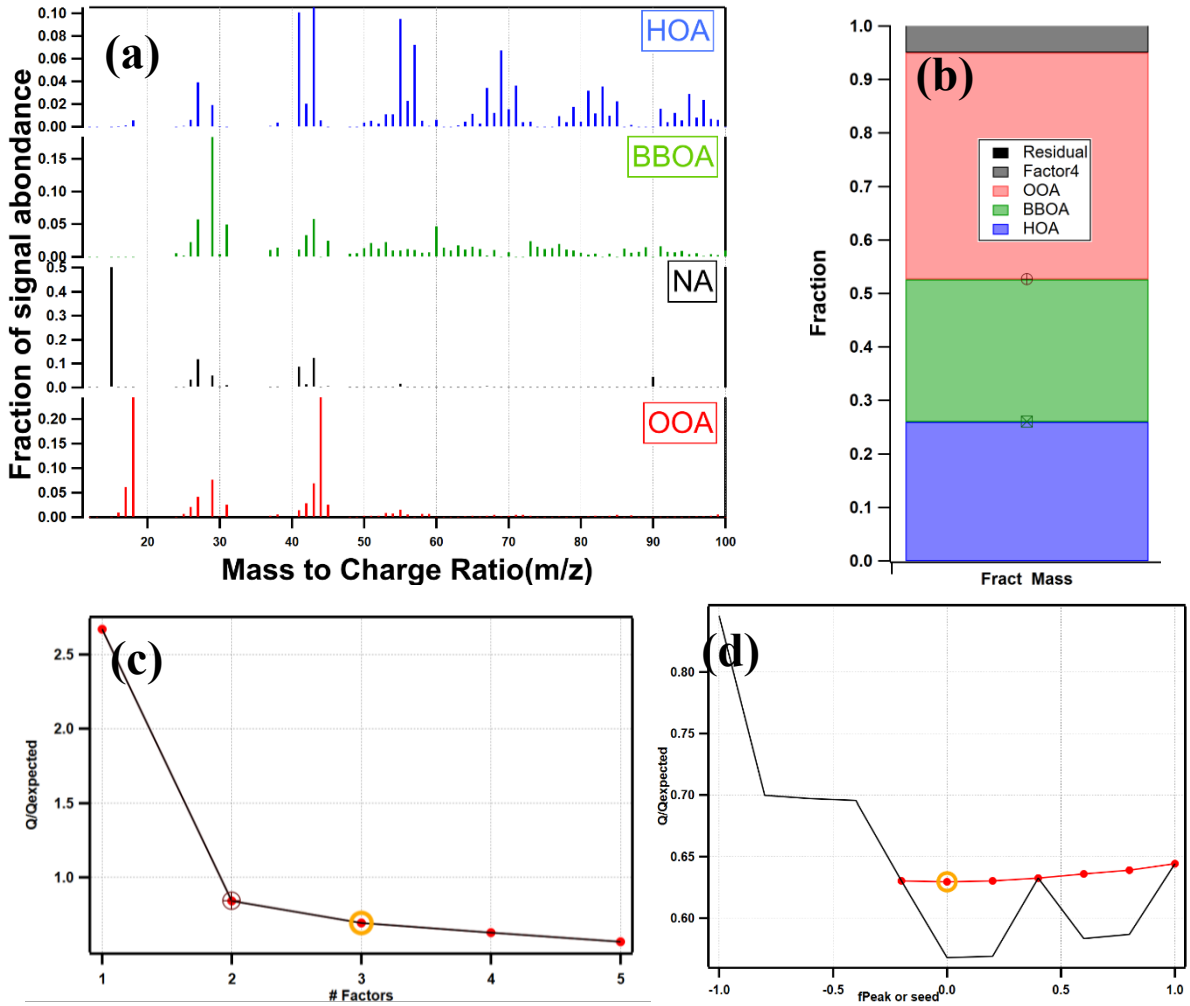

Figure S8: Organic-only PMF output. Panel (a) shows the source profiles for a 4-factor solution, and panel (b) shows the mass fraction attributed to the individual factor. Panel (c) shows the Q/Qexp as a function of the number of factors, and Panel (d) shows how Q/Qexp changes with peak for the three-factor solution.

Three-factor source profiles were selected as the most suitable PMF solutions with FPEAK = 0. The solution was chosen based on the individual source-normalized contribution to the overall mass loading, the total sum of the square of the scaled residuals (Q) to the expected ratio (Qexp), the comparison of

source spectra to standard spectra, as well as the residual factor and the correlation between R_ time series and R_ spectra.

With a three-factor solution at FPEAK = 0, the Q/Qexp value was 0.6936, compared to 0.84349 for a two-factor PMF solution. In the four-factor solution, the Q/Qexp value further decreased to 0.62963, indicating no significant improvement in source separation at the station.

The two-factor solution resolved an OOA factor and a mixed HOA+BBOA factor. This solution was not selected because both biomass burning and vehicle emissions (HOA) are expected to be important sources in Kigali.

In the four-factor solution, the deconvolved sources were OOA accounted for 42%, BBOA for 27%, HOA for 26%, and the fourth factor contributed only 6% of the total PM_1 mass. The remaining 1% was residual. Noting that a source profile is considered significant if it contributes at least 10% of the total mass load(Paatero and Tapper, 1994; Reff et al., 2007), and the fact that the fourth factor in the four-factor solution did not resemble any standard source profile and remained unstable across seasons, the three-factor solution was considered.

S4. Comparison of PMF source profiles with the external measurement and tracer ions.

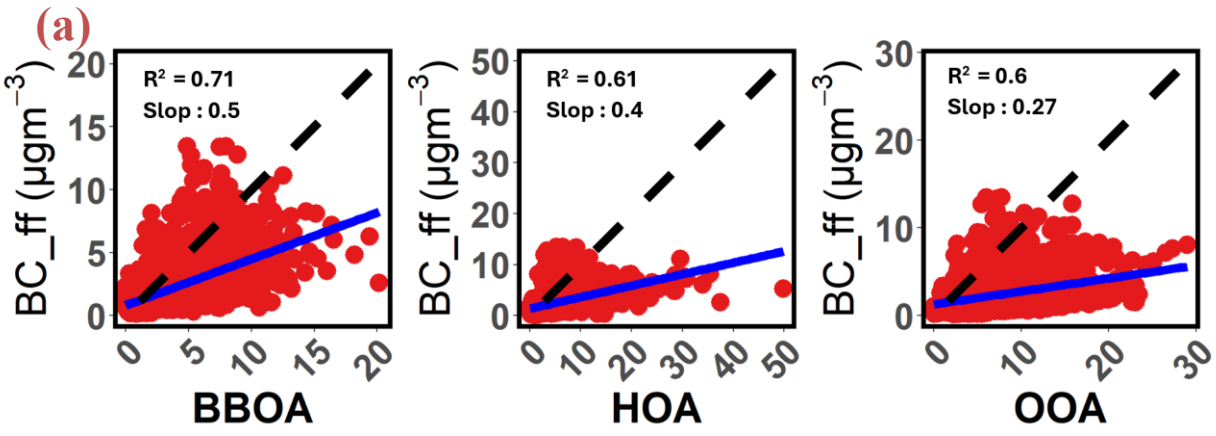

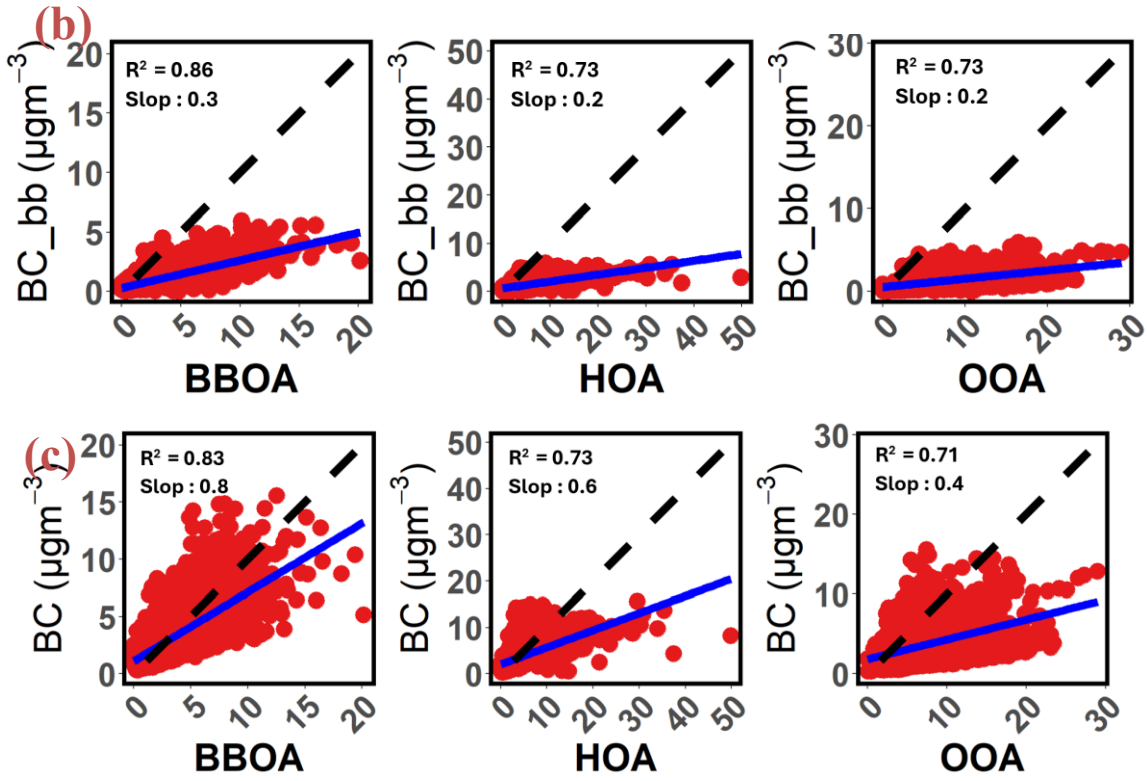

Figure S9: Comparison of the ambient measurements and delivered source profiles. ((a) BC fraction from fossil fuel combustion vs source profiles , (b) BC from Biomass burning fraction vs source profiles , (c) total black carbon vs source profiles with the)

Comparison of the source profiles' spectra and the reference spectra in the literature(Colorado state university, 2025).

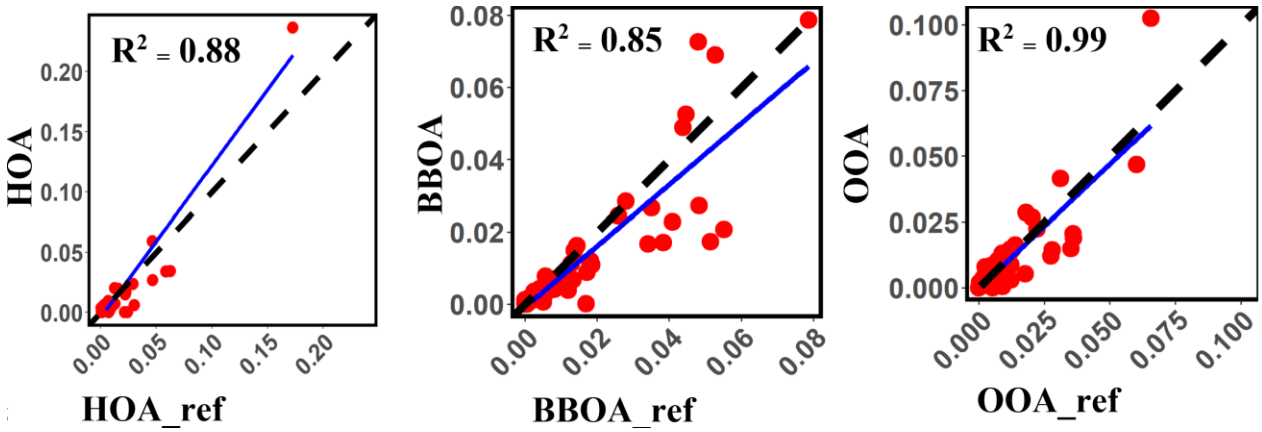

Figure S10: Source profiles spectra vs standard spectra(from left to right: (HOA Vs HOA_ref, BBOA Vs _BBOA_ref, OOA Vs OOA_ref)). All the delivered source profiles strongly correlate with the reference mass spectra.

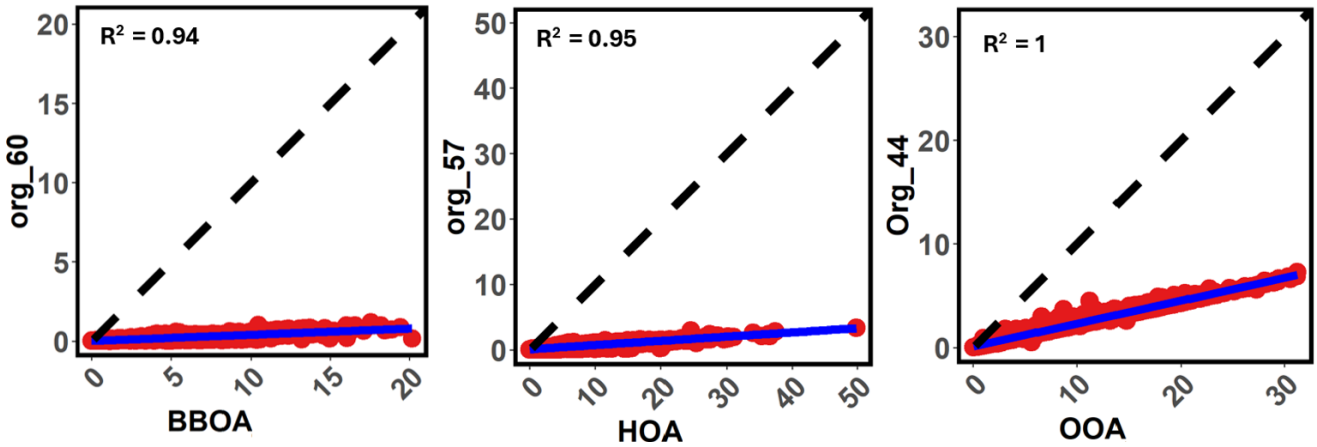

Figure S11: Source profiles vs the tracer ions. All the delivered source profiles correlate well with the individual average mass concentrations of the tracer ions (from left to right: mz60 vs BBOA, mz57 vs HOA, , and mz44 vs OOA)

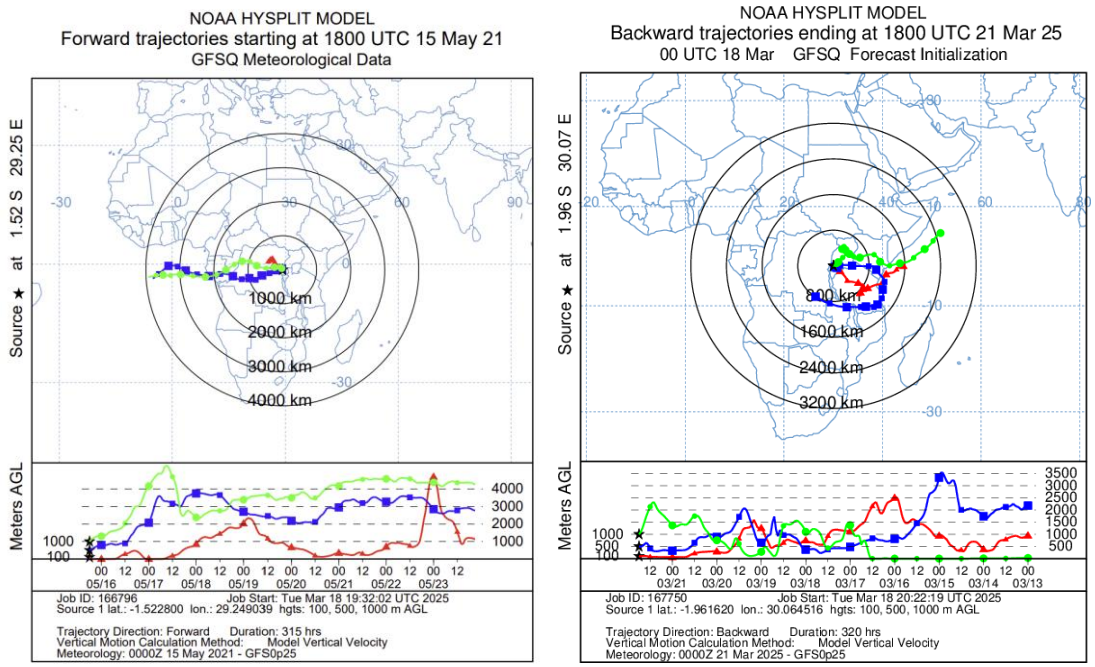

Figure S12: Forward trajectory at Nyiragogongo volcano and backward trajectory analysis of the air masses in Kigali during the recent Nyiragongo volcano eruption.

The forward trajectory analysis using the NOAA HYSPLIT model indicates that the emissions of Nyiragongo are transported in the west and no air emissions are transported to the Rwanda side. Similarly, using the back-trajectory analysis using the same model at the Kigali measurement site indicates that the station receives easterly wind originating from the eastern region of the station.

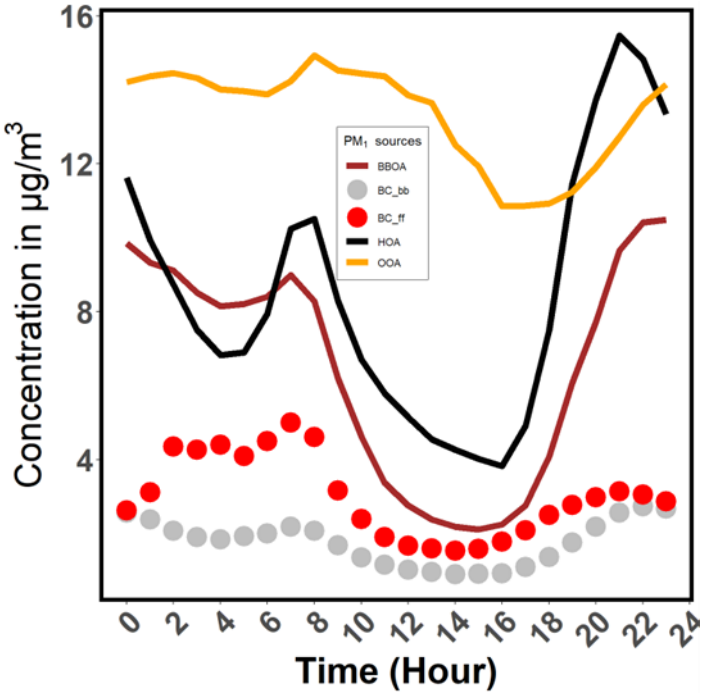

Figure S 13: Year-long diurnal patterns of PMF-derived organic PM_1 sources.

Car-free day and community works initiatives' impact on the PM absolute mass concentration, composition, and PM sources as well.

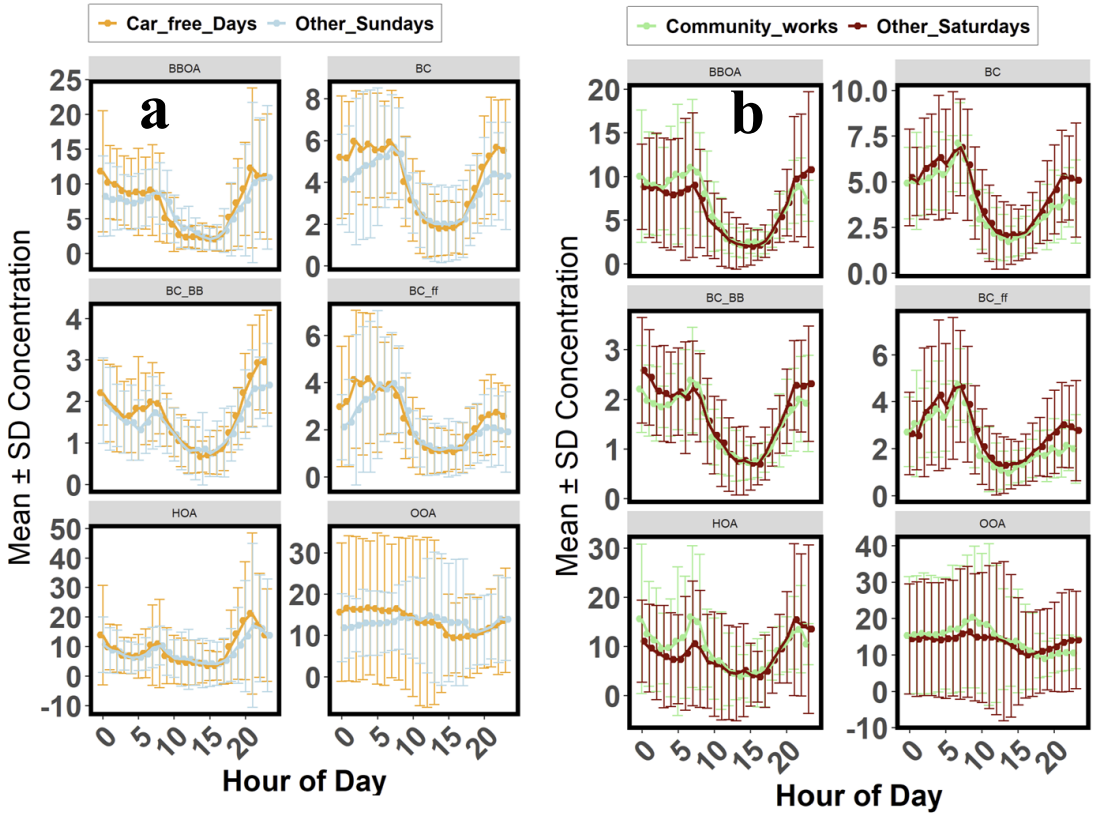

Figure S 14: Car free day and community work diurnal trend: (a) Annual mean diurnal trends of PM sources (BBOA, BC, BC_bb, BC_ff, HOA, and OOA) during car-free days over the course of one year (12 months). (b) Seasonal diurnal trends of the same PM sources during community work events.

Car-free days and community workdays consistently exhibit lower mean concentrations across most pollutants, during the internation period (car free and community work period) 07:00–11:00. However, despite the typical influence of planetary boundary layer height (PBLH), pollutant levels and source-related tracers tend to increase compared to the trend during the regular Sundays during evening hours following intervention periods, suggesting a rebound effect likely driven by intensified post-event urban activities. A similar behavior was also observed during the community work, except the no rebound in the afternoon period.

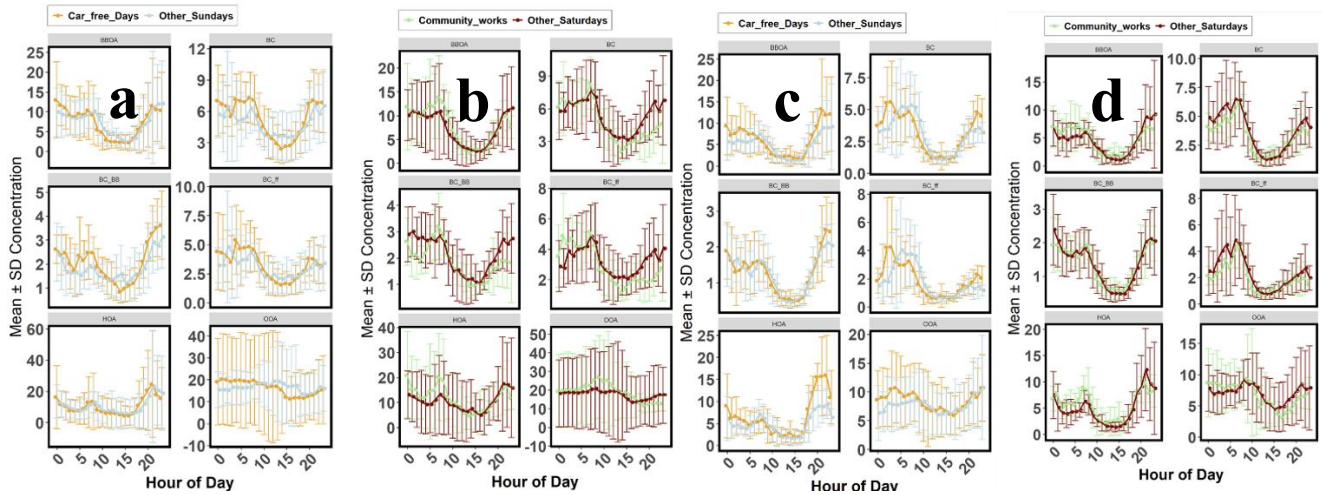

Figure S 15: Diurnal trends of PM sources (BBOA, BC, BC_bb, BC_ff, HOA, and OOA) for (a) car-free days and (b) community work events during the dry season(JJA and DJF), and (c) car-free days and (d) community work trends during the rainy season(MAM and SON).

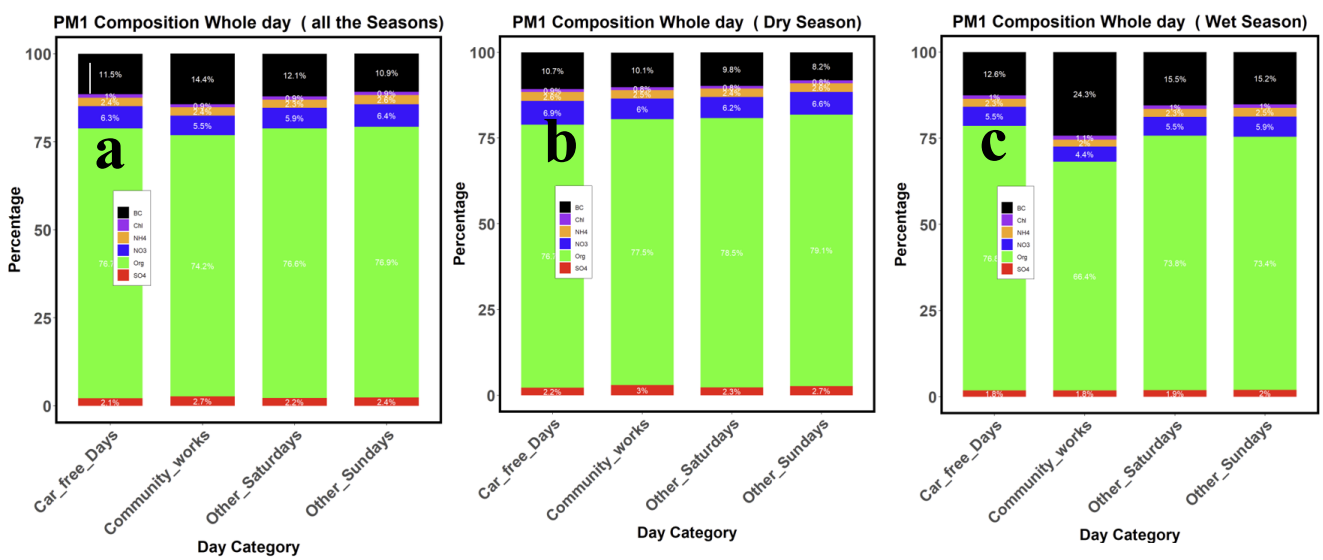

Figure S 16: Daily mean relative contribution of the PM_1 components, (a) over the courses of the year, (b) during the dry season, and (c) during the rainy season. The y-axis represents the relative contribution (%) of each component, while the x-axis shows seasonal variations. Car-free days correspond to the first and third Sundays of each month, with "Other Sundays" representing the mean of all remaining Sundays.

Community workdays correspond to the last Saturday of each month, while "Other Saturdays" represent the mean of all remaining Saturdays.

In the dry season, Car-free Days show slightly lower black carbon (BC) contributions (11.4%) compared to Other Sundays (7.4%), while organic aerosols (Org) remain nearly stable (75.4% vs. 78.2%). In the wet season, Community Workdays show a sharp rise in BC (25.1%) versus Other Saturdays (16.7%), accompanied by a drop in Org from 71.2% to 64.6%, suggesting increased combustion-related activities during community interventions.

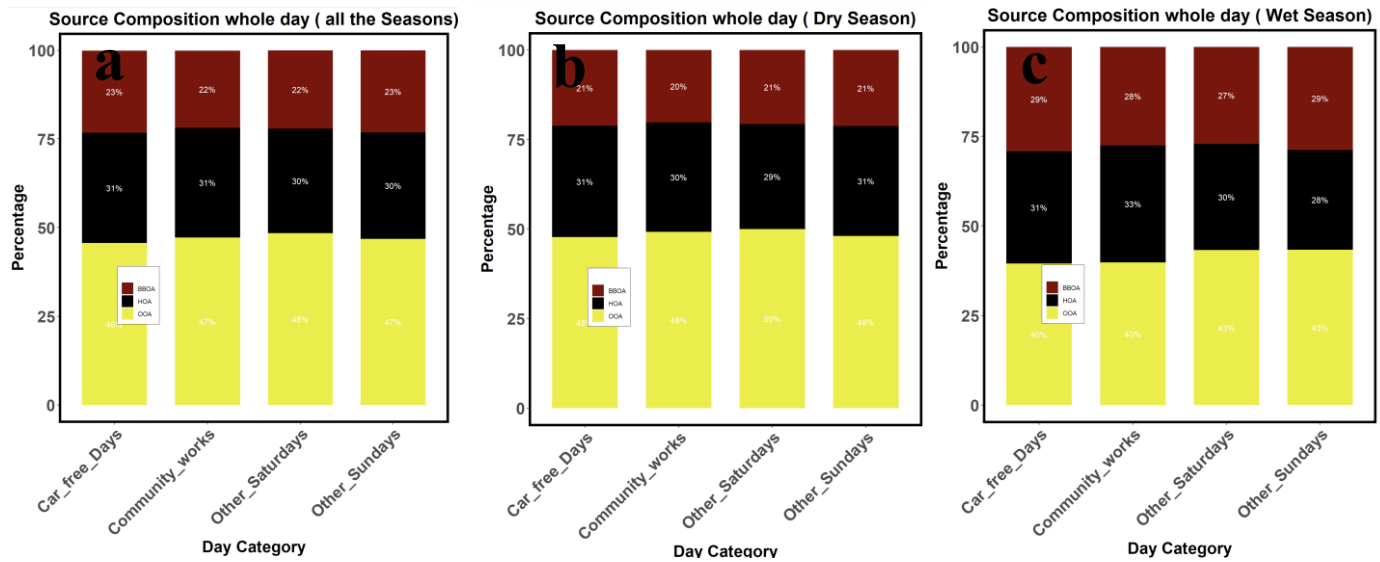

Figure S 17: Daily mean rerative PMF sources contribution on PM_1 mass loading, (a) as cources of the year, (b) during the dry season and (c) during the rainy season.

In all the seasons and on the course of the year, Car-free Days exhibited modest reductions in both HOA (−1%) and BBOA (−3%) compared to Other Sundays, suggesting slightly lower traffic and biomass burning activity. In contrast, Community Workdays showed a +2% increase in HOA relative to Other Saturdays, while BBOA contributions remained similar. Notably, source composition variability was more pronounced during the wet season, indicating greater influence of meteorological factors on emission figure S17.

Seasonal median ratios for PM absolute mass and sources during the car-free vs regular Sundays and last Saturday of each month vs regular Saturdays

Seasonal median ratios (Car-free vs. regular Sundays and Community Work vs. regular Saturdays) for full day and enforcement period (08:00–11:00) are indicated in Table 1. Ratios < 1 indicate a reduction relative to baseline days, while ratios > 1 indicate enhancement.

$$\textbf{Ratio} = \frac{\textbf{MCF}}{\textbf{MOS}} \quad \textbf{or Ratio} = \frac{\textbf{MCW}}{\textbf{MOS}} \qquad \textbf{(S2)}$$

MOS: Media of Other Sundays or other Saturdays' concentrations.

MCW: Median of all the community workday concentrations

MCF: Median of all car-free Days concentration.

Table S1: Car-free vs regular Sundays and Community work period vs regular Saturdays for both full days and the enforcement period.

Season / Species	Car-free Full Day	Community Work Full Day	Car-free Enforcement (08:00–11:00)	Community Work Enforcement (08:00–11:00)
All Seasons (12 months)				
Total PM_1	0.99	1.01	0.85	1.15
$PM_{2.5}$	1.07	1.17	0.96	0.98
BBOA	0.9525	1.0865	0.4842	1.5168
BC	1.2251	0.8770	0.8911	1.1780
BC_BB	1.0824	0.9057	1.0449	1.0821
BC_ff	1.2655	0.9149	0.9992	1.1391
HOA	1.1856	1.3017	0.8318	1.5233
OOA	0.8430	1.2210	0.7160	1.4356

Dry Season				
Total PM_1	0.98	1.01	0.84	1.38
$PM_{2.5}$	0.98	1.02	0.96	0.95
BBOA	0.9817	1.0291	0.6458	2.0592
BC	1.0660	0.8755	1.0985	1.2808
BC_BB	1.0271	0.8719	1.0971	1.3472
BC_ff	0.9551	1.1715	1.1374	1.3784
HOA	1.0874	1.3245	0.8872	1.3252
OOA	0.8767	1.1720	0.7034	1.3584
Wet Season				
Total PM_1	1	1	0.85	1.15
$PM_{2.5}$	1.07	1.17	1.03	0.97
BBOA	1.0246	1.1539	0.6349	1.2362
BC	1.1769	0.8484	0.9034	1.2307
BC_BB	1.2096	0.6797	1.0527	1.1389
BC_ff	1.1920	1.6427	1.0425	1.2076
HOA	1.2060	1.2925	0.9340	1.3377
OOA	1.0207	1.1782	0.7532	1.3855

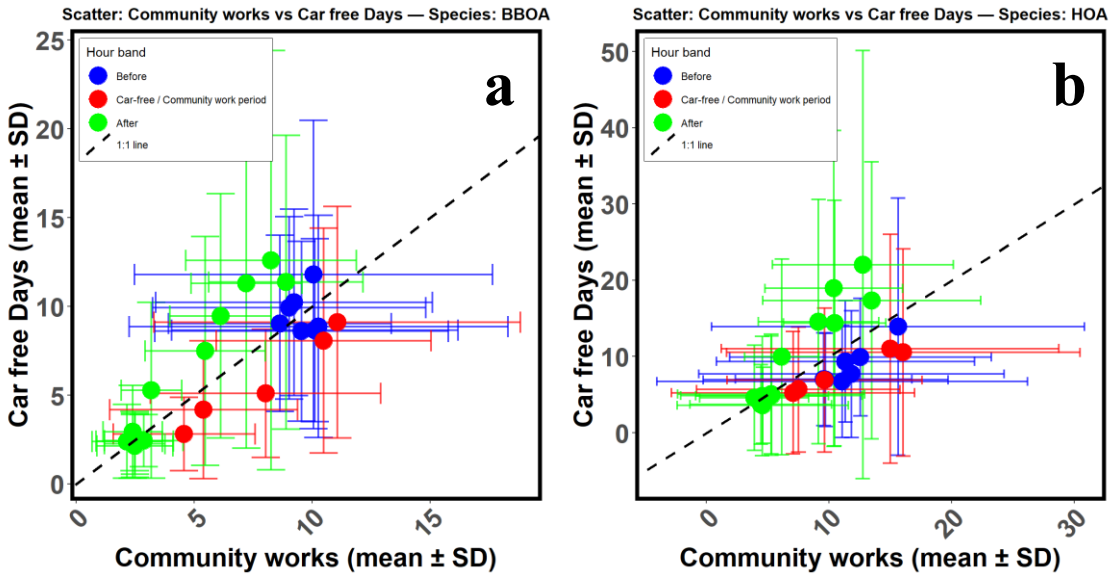

S 18: Carfree day hourly mean vs community works hourly mean in the Kigali PM measurements panel (a)for BBOA and panel (b) HOA PMF factor solutions.

Reference

Day, D. A., Campuzano-Jost, P., Nault, B. A., Palm, B. B., Hu, W., Guo, H., Wooldridge, P. J., Cohen, R. C., Docherty, K. S., Huffman, J. A., Sá, S. S. D., Martin, S. T., and Jimenez, J. L.: A systematic re-evaluation of methods for quantification of bulk particle-phase organic nitrates using real-Time aerosol mass spectrometry, Atmospheric Measurement Techniques, 15, 459–483, https://doi.org/10.5194/amt-15-459-2022, 2022.

Farmer, D. K., Matsunaga, A., Docherty, K. S., Surratt, J. D., Seinfeld, J. H., Ziemann, P. J., and Jimenez, J. L.: Response of an aerosol mass spectrometer to organonitrates and organosulfates and implications for atmospheric chemistry, Proc. Natl. Acad. Sci. U.S.A., 107, 6670–6675, https://doi.org/10.1073/pnas.0912340107, 2010.

Fry, J. L.: Organic nitrate and secondary organic aerosol yield from NO3 oxidation of β-pinene evaluated using a gas-phase kinetics/aerosol partitioning model, 2009.

Climatology of eastern Africa: http://maproom.meteorwanda.gov.rw/maproom/, last access: 30 July 2025.

Paatero, P. and Tapper, U.: Positive matrix factorization: A non-negative factor model with optimal utilization of error estimates of data values, Environmetrics, 5, 111–126, https://doi.org/10.1002/env.3170050203, 1994.

Reff, A., Eberly, S. I., and Bhave, P. V.: Receptor modeling of ambient particulate matter data using positive matrix factorization: Review of existing methods, Journal of the Air and Waste Management Association, 57, 146–154, https://doi.org/10.1080/10473289.2007.10465319, 2007.

The World Bank Group.: Rwanda Climate risk country profile, The World Bank, Rwanda, 2021.